ORIGINAL ARTICLE

Temporal trajectories of in vivo tau and amyloid-β accumulation in Alzheimer's disease

Min Seok Baek[1] · Hanna Cho[1] · Hye Sun Lee[2] · Jae Yong Choi[3,4] · Jae Hoon Lee[3] · Young Hoon Ryu[3] · Myung Sik Lee[1] · Chul Hyoung Lyoo[1]

Abstract

Purpose To investigate the temporal trajectories of tau and amyloid-β (Aβ) accumulation in Alzheimer's disease (AD) by using the longitudinal positron emission tomography (PET) study.

Methods A total of 132 participants, who were healthy volunteers or recruited in our memory disorder clinic, completed longitudinal ^{18}F-flortaucipir and ^{18}F-florbetaben PET studies with a mean follow-up time of 2 years. Referencing baseline data from 57 Aβ-negative cognitively unimpaired individuals, Z-scores and their annual changes were calculated with the global cortical or regional standardized uptake value ratios measured at baseline and follow-up after correcting for partial volume effect. The temporal trajectories of tau and Aβ burden as a function of time were obtained based on the spline models from the annual changes and baseline Z-score data.

Results Tau burden first emerged in the Braak's stage I–II regions, followed by stage III–IV regions, and finally in the stage V–VI regions. Time intervals between two time points at which Z-score curves rose above 2 were 17.3 years for the stages I–II and III–IV and 15.2 years for the stages III–IV and V–VI. Rise in the tau curve for stages I–II preceded that for global cortical Aβ, while the rise in global cortical Aβ curve preceded that for global cortical tau. Aβ accumulation rate was attenuated during the surge in tau burden in the global cortex and reached a plateau.

Conclusion Sequential appearance of Aβ and tau accumulation supports a hypothetical dynamic biomarker model and Braak's hierarchical tau spreading model in AD.

Keywords Alzheimer's disease · Positron emission tomography · Tau · ^{18}F-flortaucipir

---

Min Seok Baek and Hanna Cho contributed equally to this work.

This article is part of the Topical Collection on *Neurology*

✉ Chul Hyoung Lyoo
  lyoochel@yuhs.ac

✉ Young Hoon Ryu
  ryuyh@yuhs.ac

1 Department of Neurology, Gangnam Severance Hospital, Yonsei University College of Medicine, Seoul, South Korea

2 Biostatistics Collaboration Unit, Yonsei University College of Medicine, Seoul, South Korea

3 Department of Nuclear Medicine, Gangnam Severance Hospital, Yonsei University College of Medicine, Seoul, South Korea

4 Division of RI-Convergence Research, Korea Institute Radiological and Medical Sciences, Seoul, South Korea

Introduction

Amyloid-β (Aβ) and tau are two major pathological proteins that accumulate in the brains of Alzheimer's disease (AD). Postmortem pathological studies have revealed an early appearance and saturation of Aβ pathology and a later appearance and continuous accumulation of tau pathology throughout the disease course [1, 2]. Conventional cerebrospinal fluid (CSF) biomarkers for these two pathological proteins reflecting the amount of each pathology in the brain exhibited similar dynamics [3]. The early occurrence and plateau in the reduction of CSF $A\beta_{42}$ and later elevation of CSF total tau (t-tau) or hyperphosphorylated tau (p-tau) levels were predicted by cross-sectional studies [3–5] and later confirmed by the longitudinal studies [6–9]. CSF biomarkers have since played an important role in the diagnosis of AD and in the prediction of clinical conversion to AD dementia [10, 11]. With the development of radiotracers that selectively bind to Aβ and tau, the visualization and monitoring of the temporal and spatial progression of two pathological proteins are enabled by in vivo positron emission tomography (PET) imaging studies, showing similar dynamics to the CSF biomarkers [12–17].

A longitudinal CSF biomarker study revealed a U-shaped curve between the baseline CSF $A\beta_{42}$ levels and its annual changes, and thereby the temporal trajectory of CSF $A\beta_{42}$ estimated by the integral of annual changes in CSF $A\beta_{42}$ levels based on its baseline levels showed a sigmoid appearance with a plateau [7]. Using the same method, two longitudinal ^{11}C-Pittsburgh compound B (PIB) studies showed similar sigmoid temporal trajectories for ^{11}C-PIB standardized uptake value ratio (SUVR) with a plateau [18, 19].

Recently, four longitudinal ^{18}F-flortaucipir studies have observed progressive tau accumulation in AD patients [16, 17, 20, 21], but temporal trajectory of tau was not assessed. In this study, we sought to investigate the temporal trajectories of Aβ and tau by using longitudinal data from ^{18}F-florbetaben and ^{18}F-flortaucipir PET studies. Additionally, trajectories of tau accumulation in the regions for different tau stages were separately analyzed to determine whether there is a temporal sequence of tau accumulation in the regions for advancing tau stages.

Materials and methods

Participants

We included 132 individuals who completed baseline tau PET study at Gangnam Severance Hospital from January 2015 to December 2016 and agreed to participate in this follow-up study. At baseline, two PET scans (^{18}F-flortaucipir for tau and ^{18}F-florbetaben for Aβ), magnetic resonance (MR) imaging studies, and neuropsychological tests (Seoul

Neuropsychological Screening Battery including tests for global cognition and 6 cognitive domains) were conducted [22], as described in our previous study [14]. Based on the neuropsychological test results and amyloid-positivity decided by the two nuclear medicine specialists by using the validated visual assessment methods [23, 24], baseline clinical diagnoses were made using the diagnostic criteria proposed by the National Institute on Aging-Alzheimer's Association [25, 26]. AD dementia (DEM) was diagnosed using the criteria for "Probable AD dementia with evidence of the AD pathophysiological process" and prodromal AD (mild cognitive impairment; MCI) with the criteria for "MCI due to AD with intermediate or high likelihood". We also included cognitively unimpaired (CU) individuals who showed no subjective memory complaint, normal performances in baseline neuropsychological tests, and no abnormalities in brain MR imaging. Finally, 132 individuals were classified into four diagnostic groups [57 Aβ-negative CU (CU−), 7 Aβ-positive CU (CU+), 39 Aβ-positive MCI (MCI+), and 29 Aβ-positive DEM (DEM+)]. For the follow-up study, all participants underwent the same assessments that were conducted in the baseline study.

Image processing steps

Freesurfer 5.3 (Massachusetts General Hospital, Harvard Medical School; http://surfer.nmr.mgh.harvard.edu) software was used to create participant-specific volumes-of-interest (VOIs) as described in our previous study [14]. After merging anatomically related regions in both sides in 112 cortical and subcortical segments, participant-specific VOI mask images including 25 cortical and 5 subcortical (thalamus, caudate, putamen, pallidum, and cerebellar cortex) regions were created within FreeSurfer space ($256 \times 256 \times 256$ matrix with 1 mm isovoxels). The voxel counts in each region were considered to be regional volumes.

We used statistical parametric mapping 12 (Wellcome Trust Centre for Neuroimaging, London, UK) and in-house software implemented in MATLAB 2015b (MathWorks, Natick, MA, USA) to achieve integrative analysis of the multimodal images. First, PET images were coregistered to individual MR images within FreeSurfer space and then were corrected for partial volume effect (PVE) by using the VOI mask images with the region-based voxel-wise method [27]. To minimize the contamination from neighboring basal temporal and occipital cortices, we created SUVR images with the cerebellar crus median obtained from spatially normalized PET images as a reference. Finally, regional SUVR values were measured by overlaying participant-specific VOI masks on the SUVR images. To obtain the main trajectories of tau and Aβ, we primarily measured global cortical SUVR values for ^{18}F-flortaucipir and ^{18}F-florbetaben PET. For ^{18}F-flortaucipir PET, we also measured the SUVR values for the

regions corresponding to the Braak's stages I–II (entorhinal cortex and hippocampus), III–IV (amygdala, parahippocampal, fusiform, lingual, inferior and middle temporal, and insula cortices), and V–VI (orbitofrontal, superior, middle and inferior frontal, precentral, paracentral, postcentral, precuneus, inferior and superior parietal, supramarginal, superior temporal, medial and lateral occipital, and anterior and posterior cingulate cortices) by volume-weighted averaging.

Trajectory analysis

We used an in-house program implemented in MATLAB for trajectory analysis with the same method that was used to determine the temporal trajectory of the biomarkers [7, 18, 19]. For the temporal synchronization of tau and Aβ curves, baseline and follow-up SUVR values were converted to Z-scores with reference to the baseline data from 57 CU− individuals, and then the annual changes in Z-scores were calculated. The trajectories of annual changes in Z-scores (ΔZ/year) as a function of baseline Z-scores were obtained using the restricted cubic spline model with knots on Z-scores 0, 5, 10, 15, and 20 for ^{18}F-florbetaben and on Z-scores 0, 2, 4, and 8 for ^{18}F-flortaucipir PET. For the tau stage III–IV region, we used an additional knot on Z-score 12. We finally obtained predicted Z-score curves as a function of time in year by using the modified Euler's method for solving the first-order differential equation with time 0 anchored to Z-score 0. For additional analysis, we selected 14 CU− individuals whose baseline SUVR values in the composite region for Braak's stage I–II were within first quartile of the entire 57 CU− individuals and then repeated same trajectory analysis with the Z-scores calculated with these 14 CU− individuals who were considered to be least affected by the tau pathology.

Statistical analysis

SPSS 23 (IBM Corp., Armonk, NY, USA) was used for the statistical analysis of demographic data and cognitive function tests. For between-group comparisons, one-way ANOVA (with post hoc tests) was used for continuous variables and the Chi-square test was used for categorical variables. Multiple comparisons were corrected for by Bonferroni's method. In order to check the longitudinal changes in cognitive function within each group, we used a linear mixed effect model in MATLAB with age, gender, years of education, and presence of ApoE ε4 allele as fixed factors under the assumption of random intercept and slope.

Results

Demographic characteristics and neuropsychological tests

Demographic data are summarized in Table 1. Compared to the CU− group, the mean age at baseline was older and the mean follow-up interval was shorter in the MCI+ and DEM+ groups. Disease duration was longer in the DEM+ than in the MCI+ group. Apolipoprotein E ε4 allele was more frequently observed in the MCI+ and DEM+ groups than in the CU− group, while there were no differences in gender distribution and years of education between the groups after correcting for multiple comparisons. The mean time interval between the baseline and follow-up for all participants was 24.0 ± 2.1 months, and the time interval was shorter in MCI+ and DEM+ than that in CU−. During the follow-up period, global cognition as determined by Mini-Mental State Examination (MMSE) and Clinical Dementia Rating sum-of-boxes (CDR-SB) scores worsened in the CU−, MCI+, and DEM+ groups.

Tau and Aβ accumulation rates and their baseline levels

Global cortical Aβ accumulation rate increased until the baseline Z-score reached 12.8 and then subsequently decreased even below 0 after the baseline Z-score 19.8. Thereby, the curve for the Aβ accumulation rate as a function of baseline Aβ Z-score showed an inverted U-shape (Fig. 1a). In contrast, the global cortical tau accumulation rate started to increase around the baseline Z-score 1 and steadily increased thereafter (Fig. 1b and f). Similar to the global cortical tau accumulation rate, the tau accumulation rate in the regions for Braak's stage III–IV and V–VI also increased above baseline Z-score 1 (Fig. 1d–f). Unlike these patterns, the tau accumulation rate in the regions for Braak's stage I–II showed a steady increase even at very low baseline Z-scores (Fig. 1c and f).

The results of curve fitting with the Z-score data calculated with the 14 CU− individuals least affected by the tau pathology showed similar inverted U-shaped Aβ accumulation rate curve and steadily increasing tau accumulation rate curves for each Braak's stage region. Unlike these Braak's stage regions, the curve for global cortical tau accumulation rate bent downward at the extremely high baseline tau burden (Supplementary Fig. 1).

Temporal trajectories of in vivo tau and Aβ burden

The temporal trajectories of tau and Aβ burden are shown in Fig. 2. Global cortical Aβ burden steadily increased until it slowly approached a plateau around the time point of 40 years, and thereby its trajectory as a function of time showed sigmoid

Table 1 Baseline demographic characteristics and changes in cognitive functions

	CU−		CU+		MCI+		DEM+	
n	57		7		39		29	
Baseline age (years)	65.9 ± 9.7		71.7 ± 4.2		73.9 ± 6.1[a]		72.7 ± 9.7[a]	
Gender (M/F)	23: 34		3: 4		20: 19		6: 23	
Education (years)	12.3 ± 4.6		13.0 ± 4.1		11.5 ± 4.5		10.0 ± 5.6	
Duration (years)	n.a.		n.a.		2.5 ± 1.3		3.6 ± 1.3[c]	
ApoE ε4+ (ε4+:ε4-)	9: 48 (15%)		2: 5 (29%)		20: 19 (51%)[a]		18: 11 (62%)[a]	
Interval (months)	24.9 ± 2.3		24.4 ± 1.9		23.2 ± 1.5[a]		23.0 ± 1.4[a]	
Cognitive function	**baseline**	**follow-up**	**baseline**	**follow-up**	**baseline**	**follow-up**	**baseline**	**follow-up**
MMSE	28.3 ± 1.7	27.4 ± 3.0[*]	28.1 ± 2.1	27.3 ± 2.9	25.0 ± 3.4[a]	22.5 ± 4.5[ab*]	19.6 ± 4.5[abc]	16.7 ± 5.4[abc*]
CDR-SB	0.0 ± 0.0	0.7 ± 0.8[*]	0.0 ± 0.0	0.7 ± 1.1	1.8 ± 0.9[ab]	3.1 ± 1.8[ab*]	4.5 ± 1.8[abc]	6.5 ± 3.0[abc*]

Data are presented as mean ± SD. Intervals represent the time interval between baseline and follow-up

[a] $P < 0.05$ for the comparisons between the CU− and each group

[b] $P < 0.05$ for the comparisons between the CU+ and MCI/DEM+ groups

[c] $P < 0.05$ for the comparisons between the MCI+ and DEM+ groups

[*] $P < 0.05$ for significant changes between baseline and follow-up

CU cognitively unimpaired, *MCI* mild cognitive impairment, *DEM* dementia, ± Aβ-positivity, *ApoE* apolipoprotein E, *MMSE* Mini-Mental State Examination, *CDR-SB* Clinical Dementia Rating sum-of-boxes, *n.a.* not applicable or not available

appearance. Global cortical tau burden increased relatively more slowly until the time point of 30 years before showing a rapid increase around the time point of 35 years without reaching plateau. Similar exponential tau trajectories were observed in the composite subregions for Braak's stages I–II, III–IV, and V–VI. The surge in tau burden first appeared in the regions for stage I–II and was then followed by a surge in the regions for stage III–IV around the time point of 30 years.

When we selected a Z-score 2 as a cut-off for determining abnormally increased tau and Aβ burden, the global cortical Aβ burden reached the cut-off Z-score at the time point of 16.2 years, and subsequently after 16.2 years, global cortical tau burden reached cut-off Z-score. Even prior to the rise of Aβ above the cut-off, tau burden in the regions for stage I–II reached the cut-off Z-score at the time point of 13.3 years. The time interval between the time points for increased tau burden in the regions for stages I–II and III–IV was 17.3 years, and that between the time points for increased tau burden in the regions for stage III–IV and V–VI was 15.2 years.

Trajectory curves derived with the Z-score data calculated with the 14 CU− individuals least affected by the tau pathology exhibited almost similar pattern, but the time points exceeding cut-off Z-score 2 appeared earlier than those obtained above (Supplementary Fig. 2).

Discussion

In this longitudinal PET study modeling the temporal trajectories of Aβ and tau burden, the time point at which the Aβ curve rose above the Z-score 2 preceded the time point at

which the global cortical tau curve rose above Z-score 2 by 16.2 years. Rise in the tau curve occurred sequentially in the regions for advancing tau stages. The time intervals between the time points when the tau burden in the stages I–II, III–IV, and V–VI regions rose above Z-score 2 were 17.3 and 15.2 years, respectively. According to our model, the rise in the tau curve for the stage I–II region preceded that of the Aβ curve by about 3 years.

Saturation of neocortical Aβ pathology had been suggested in previous postmortem studies and CSF and imaging biomarker studies [1, 2, 7, 18, 19]. Likewise, the Aβ accumulation rate was attenuated and even converted to negative values in individuals with high baseline Aβ Z-scores in our data. For this reason, the Aβ accumulation rate curve as a function of baseline Z-scores showed an inverted U-shape and the integral of the annual change in Aβ Z-scores based on the baseline values showed a sigmoid appearance with a plateau. Trajectory models for the CSF t-tau and p-tau levels suggested a plateau at a later time point similar to the Aβ curve [5, 8, 28]. Such saturation of tau pathology was suspected in the Braak's postmortem study showing the replacement of intraneuronal neurofibrillary tangles in the medial temporal cortex by ghost tangles after the neuronal death in advanced stages [29]. In contrast, CSF p-tau levels did not plateau in the individuals showing an increase in CSF p-tau in a longitudinal study modeling the trajectory of CSF biomarkers [7], and the global cortical tau Z-scores increased exponentially also without a later plateau in our study. Unlike the Aβ pathology which appears early and is likely to show its full dynamics within the neocortex prior to advanced AD, the later appearance of neocortical tau pathology may limit the observation of
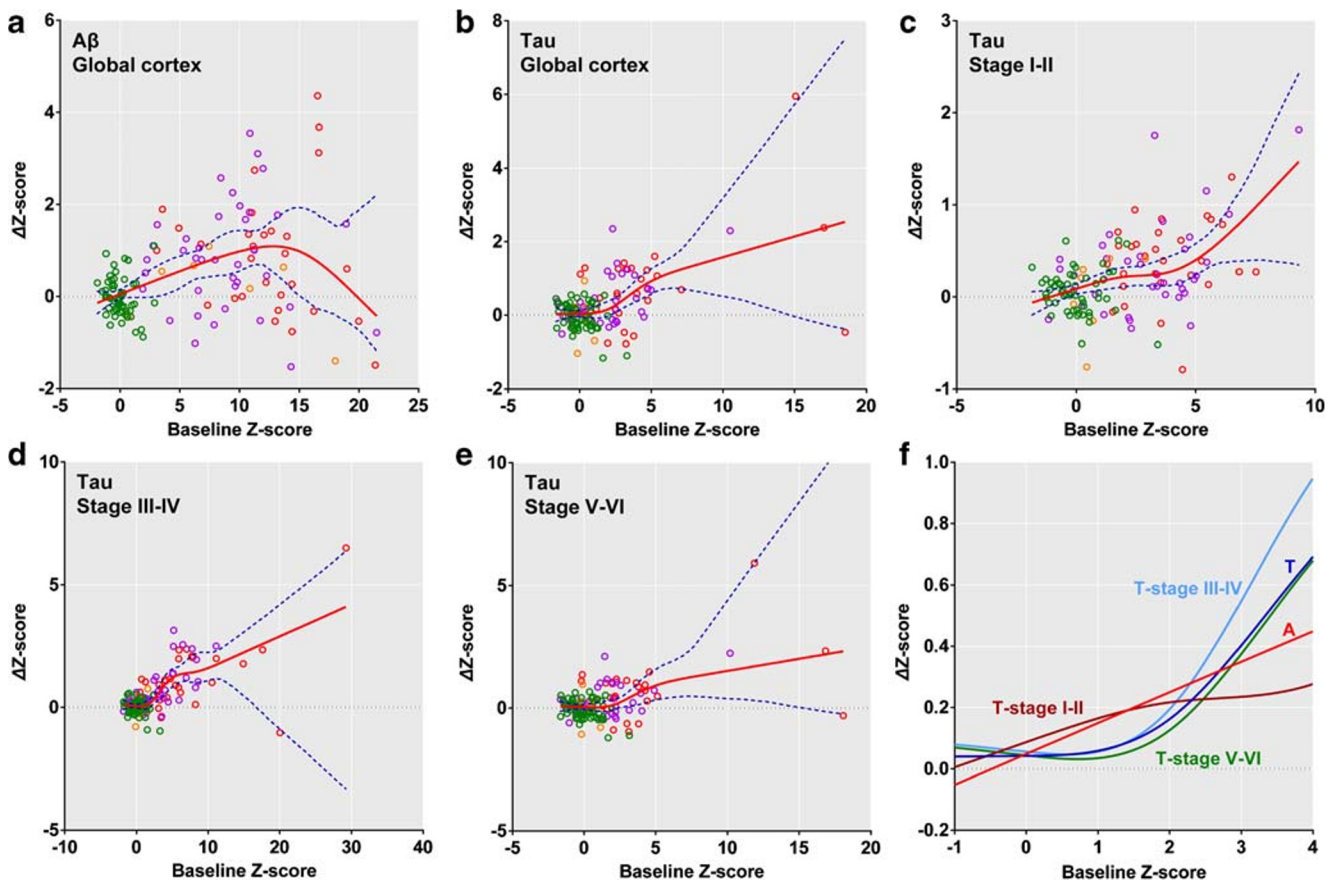
Fig. 1 Tau and Aβ accumulation rates as a function of baseline levels. In contrast to the Aβ accumulation rate which attenuates in patients with high baseline Aβ burden and thereby shows inverted U-shape curve (**a**), the curves for tau accumulation rates in various regions do not bend in such a way (**b–e**). Subplot F shows magnified curves focusing on low baseline Z-scores. Unlike the steady increase in accumulation rates of Aβ in the global cortex and tau in the regions for stage I–II, tau accumulation rates in the global cortex and the regions for stages III–VI and V–VI do not increase until a baseline Z-score 1. Blue dotted lines represent 95% confidence intervals. Green, orange, violet, and red circles represent the individuals with CU−, CU+, MCI+, and DEM+, respectively. Z-scores and their annual changes were calculated with the partial volume effect-corrected SUVR values referencing baseline data from 57 CU− individuals. Abbreviations: A = global cortical Aβ burden, T = global cortical tau burden, T-stage I–II, III–V, and V–VI = tau burden in the regions for Braak's neurofibrillary tangle stages, CU = cognitively unimpaired, MCI = mild cognitive impairment, DEM = Alzheimer's disease dementia, ± Aβ-positivity, SUVR = standardized uptake value

attenuating tau accumulation. We suspect that the absence of far advanced AD dementia patients, who would be likely to progress to show severe dementia and thereby become ineligible for imaging studies at both baseline and follow-up, might have made fitted spline curve relatively unreliable at the right side of the plot and may explain this discrepancy. Alternatively, CSF p-tau and tau burden measured by the ^{18}F-flortaucipir PET may have different dynamics. In contrast to the ^{18}F-flortaucipir PET reflecting the entire tau pathology, sequestration of p-tau in neurofibrillary tangles or neuronal death may cause a reduction in CSF p-tau and its plateauing in later stages [30].

Jack et al. estimated a time interval for the SUVR value to increase from 1.5 to 2.0 and from 2.0 to 2.5 as 6.6 and 7.7 years, respectively [18]. Based on PVE-corrected data, Villemagne et al. estimated the time required for the ^{11}C-PIB SUVR value to increase from the mean of the controls to the cut-off value for Aβ-positivity to be 8.4 years and from the

cut-off to the mean of AD patients to be 17.7 years [19]. When Z-score 2 was selected as a cut-off, our study estimated the time required for the Z-score of ^{18}F-florbetaben SUVR to rise from the Z-score 0 to 2 to be 16.2 years and from Z-score 2 to mean Z-score of AD to be 16.8 years. Our calculated time to reach Aβ Z-score 2 was close to that derived in the longitudinal CSF Aβ42 biomarker study (18.6 years) [7], but almost double that derived in the longitudinal ^{11}C-PIB PET study (8.4 years) [19].

Tau pathology initially appears in the transentorhinal and entorhinal cortices, spreading hierarchically to the neighboring medial temporal regions and subsequently to the diffuse association cortices, before finally reaching the primary cortices [29]. This pattern was replicated in our previous cross-sectional ^{18}F-flortaucipir PET studies [14, 31]. Tau curves for the stages I–II, III–IV, and V–VI regions rose sequentially in the present study, providing further evidence for the Braak's hypothetical model of tau spreading and the existence of a
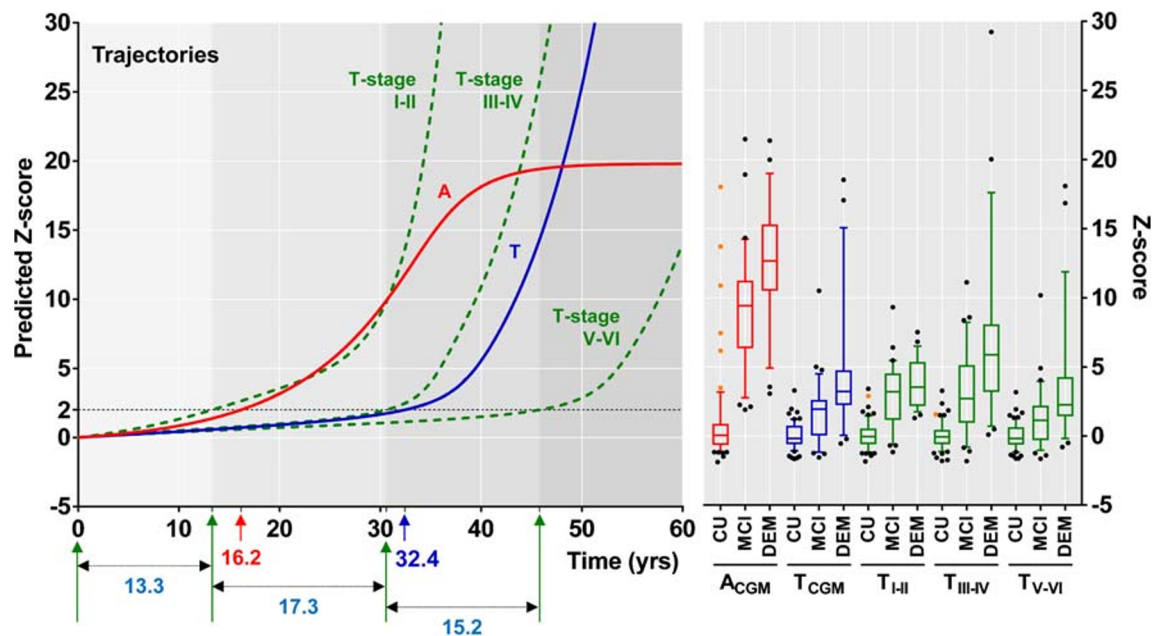
Fig. 2 Trajectories of tau and Aβ burden as a function of time. The global cortical Aβ curve reaches a plateau with a sigmoid appearance, while the global cortical tau curve shows an exponential increase around the time point at which the increase in Aβ burden approaches a plateau. Tau curves in the regions for stages I–II, III–IV, and V–VI show similar exponential increases in a sequential manner. Red and blue arrows indicate the time points at which the global Aβ and tau curves rise above Z-score 2, respectively. Box and whisker plot on the right shows baseline tau and Aβ levels in Z-scores for each group and region. Upper and lower horizontal bars represent 90th and 10th percentiles, and orange dots represent the CU+ individuals. Z-scores and their annual changes were calculated with the partial volume effect-corrected SUVR values referencing baseline data from 57 CU− individuals. Abbreviations: A = global cortical Aβ burden, T = global cortical tau burden, T-stage I–II, III–V, and V–VI = tau burden in the regions for Braak's neurofibrillary tangle stages, CU = cognitively unimpaired, MCI = mild cognitive impairment, DEM = Alzheimer's disease dementia, ± Aβ-positivity, SUVR = standardized uptake value

temporal sequence of tau accumulation. Interestingly, the tau accumulation rate in the stage I–II regions showed a steady increase even at very low baseline Z-scores, and thereby the rise in tau curves for the stage I–II regions above Z-score 2 even preceded the Aβ curve by 2.9 years like the hypothetical dynamic biomarker model suggested by Jack et al. [32]. Primary age-related tauopathy (PART) was attached to this condition: the existence of tau pathology confined to the medial temporal cortex in the absence of Aβ pathology [33]. Tau pathology identified in PART is almost identical to that in AD [33], but future progression of the elderly with PART to AD is still unknown [21, 33, 34]. When we assume that the conversion from PART to AD can be proven by tau accumulation beyond the stage I–II regions, it is interesting to note that at least 17 years of follow-up may be required to investigate this hypothesis according to our model. A longitudinal study with a much longer time period than expected may be necessary to investigate the conversion from PART to AD.

Our derived tau curve might be shifted toward the right side, because we primarily used all 57 CU− individuals who might have age-related tau accumulation in the stage I–II regions for the reference. As expected, when the individuals who were considered to be least affected by tau pathology was used for the calculation of Z-scores, the increase of Aβ and tau in the trajectory model was brought forward

(Supplementary Figs. 1 and 2). In addition, 2-year time interval might be too short to derive a life-long trajectory model, and our model might have neglected focal increase of tau burden.

In summary, sequential appearance of Aβ and tau accumulation in our temporal trajectory model supports the hypothetical dynamic biomarker model and Braak's hierarchical tau spreading model in AD.

Authors' contributions Y. H. Ryu Conception and design, Administrative support, Collection and assembly of data, Data analysis and interpretation, Supervision, Final approval of manuscript

C. H. Lyoo Conception and design, Administrative support, Collection and assembly of data, Data analysis and interpretation, Manuscript writing, Final approval of manuscript

Compliance with ethical standards

Competing interests   The authors declare that they have no competing interests.

Ethics approval and consent to participate   This study was approved by the institutional review board of Gangnam Severance Hospital and written informed consent was obtained from all participants.

References

1. Ingelsson M, Fukumoto H, Newell KL, Growdon JH, Hedley-Whyte ET, Frosch MP, et al. Early Abeta accumulation and progressive synaptic loss, gliosis, and tangle formation in AD brain. Neurology. 2004;62:925–31.

2. Markesbery WR, Schmitt FA, Kryscio RJ, Davis DG, Smith CD, Wekstein DR. Neuropathologic substrate of mild cognitive impairment. Arch Neurol. 2006;63:38–46.

3. Tapiola T, Alafuzoff I, Herukka SK, Parkkinen L, Hartikainen P, Soininen H, et al. Cerebrospinal fluid {beta}-amyloid 42 and tau proteins as biomarkers of Alzheimer-type pathologic changes in the brain. Arch Neurol. 2009;66:382–9.

4. Buchhave P, Minthon L, Zetterberg H, Wallin AK, Blennow K, Hansson O. Cerebrospinal fluid levels of beta-amyloid 1-42, but not of tau, are fully changed already 5 to 10 years before the onset of Alzheimer dementia. Arch Gen Psychiatry. 2012;69:98–106.

5. Caroli A, Frisoni GB. Alzheimer's disease neuroimaging I. The dynamics of Alzheimer's disease biomarkers in the Alzheimer's disease neuroimaging initiative cohort. Neurobiol Aging. 2010;31:1263–74.

6. Lo RY, Hubbard AE, Shaw LM, Trojanowski JQ, Petersen RC, Aisen PS, et al. Longitudinal change of biomarkers in cognitive decline. Arch Neurol. 2011;68:1257–66.

7. Toledo JB, Xie SX, Trojanowski JQ, Shaw LM. Longitudinal change in CSF tau and Abeta biomarkers for up to 48 months in ADNI. Acta Neuropathol. 2013;126:659–70.

8. Yang E, Farnum M, Lobanov V, Schultz T, Verbeeck R, Raghavan N, et al. Quantifying the pathophysiological timeline of Alzheimer's disease. J Alzheimers Dis. 2011;26:745–53.

9. Jack CR Jr, Vemuri P, Wiste HJ, Weigand SD, Aisen PS, Trojanowski JQ, et al. Evidence for ordering of Alzheimer disease biomarkers. Arch Neurol. 2011;68:1526–35.

10. Hansson O, Zetterberg H, Buchhave P, Londos E, Blennow K, Minthon L. Association between CSF biomarkers and incipient Alzheimer's disease in patients with mild cognitive impairment: a follow-up study. Lancet Neurol. 2006;5:228–34.

11. Mattsson N, Zetterberg H, Hansson O, Andreasen N, Parnetti L, Jonsson M, et al. CSF biomarkers and incipient Alzheimer disease in patients with mild cognitive impairment. JAMA. 2009;302:385–93.

12. Klunk WE, Engler H, Nordberg A, Wang Y, Blomqvist G, Holt DP, et al. Imaging brain amyloid in Alzheimer's disease with Pittsburgh compound-B. Ann Neurol. 2004;55:306–19.

13. Villain N, Chetelat G, Grassiot B, Bourgeat P, Jones G, Ellis KA, et al. Regional dynamics of amyloid-beta deposition in healthy elderly, mild cognitive impairment and Alzheimer's disease: a voxelwise PiB-PET longitudinal study. Brain. 2012;135:2126–39.

14. Cho H, Choi JY, Hwang MS, Kim YJ, Lee HM, Lee HS, et al. In vivo cortical spreading pattern of tau and amyloid in the Alzheimer disease spectrum. Ann Neurol. 2016;80:247–58.

15. Cho H, Choi JY, Hwang MS, Lee JH, Kim YJ, Lee HM, et al. Tau PET in Alzheimer disease and mild cognitive impairment. Neurology. 2016;87:375–83.

16. Jack CR Jr, Wiste HJ, Schwarz CG, Lowe VJ, Senjem ML, Vemuri P, et al. Longitudinal tau PET in ageing and Alzheimer's disease. Brain. 2018;141:1517–28.

17. Southekal S, Devous MD Sr, Kennedy I, Navitsky M, Lu M, Joshi AD, et al. Flortaucipir F 18 quantitation using parametric estimation of reference signal intensity. J Nucl Med. 2018;59:944–51.

18. Jack CR Jr, Wiste HJ, Lesnick TG, Weigand SD, Knopman DS, Vemuri P, et al. Brain beta-amyloid load approaches a plateau. Neurology. 2013;80:890–6.

19. Villemagne VL, Burnham S, Bourgeat P, Brown B, Ellis KA, Salvado O, et al. Amyloid beta deposition, neurodegeneration, and cognitive decline in sporadic Alzheimer's disease: a prospective cohort study. Lancet Neurol. 2013;12:357–67.

20. Harrison TM, La Joie R, Maass A, Baker SL, Swinnerton K, Fenton L, et al. Longitudinal tau accumulation and atrophy in aging and alzheimer disease. Ann Neurol. 2019;85:229–40.

21. Cho H, Choi JY, Lee HS, Lee JH, Ryu YH, Lee MS, et al. Progressive tau accumulation in Alzheimer disease: 2-year follow-up study. J Nucl Med. 2019;60:1611–21.

22. Kang Y, Na DL. Seoul neuropsychological screening battery (SNSB). Incheon: Human Brain Research & Consulting Co.; 2003.

23. Sabri O, Sabbagh MN, Seibyl J, Barthel H, Akatsu H, Ouchi Y, et al. Florbetaben PET imaging to detect amyloid beta plaques in Alzheimer's disease: phase 3 study. Alzheimers Dement. 2015;11:964–74.

24. Villemagne VL, Ong K, Mulligan RS, Holl G, Pejoska S, Jones G, et al. Amyloid imaging with (18)F-florbetaben in Alzheimer disease and other dementias. J Nucl Med. 2011;52:1210–7.

25. McKhann GM, Knopman DS, Chertkow H, Hyman BT, Jack CR Jr, Kawas CH, et al. The diagnosis of dementia due to Alzheimer's disease: recommendations from the National Institute on Aging-Alzheimer's Association workgroups on diagnostic guidelines for Alzheimer's disease. Alzheimers Dement. 2011;7:263–9.

26. Albert MS, DeKosky ST, Dickson D, Dubois B, Feldman HH, Fox NC, et al. The diagnosis of mild cognitive impairment due to Alzheimer's disease: recommendations from the National Institute on Aging-Alzheimer's Association workgroups on diagnostic guidelines for Alzheimer's disease. Alzheimers Dement. 2011;7:270–9.

27. Thomas BA, Erlandsson K, Modat M, Thurfjell L, Vandenberghe R, Ourselin S, et al. The importance of appropriate partial volume correction for PET quantification in Alzheimer's disease. Eur J Nucl Med Mol Imaging. 2011;38:1104–19.

28. Donohue MC, Jacqmin-Gadda H, Le Goff M, Thomas RG, Raman R, Gamst AC, et al. Estimating long-term multivariate progression from short-term data. Alzheimers Dement. 2014;10:S400–10.

29. Braak H, Braak E. Neuropathological stageing of Alzheimer-related changes. Acta Neuropathol. 1991;82:239–59.

30. La Joie R, Bejanin A, Fagan AM, Ayakta N, Baker SL, Bourakova V, et al. Associations between [(18)F]AV1451 tau PET and CSF measures of tau pathology in a clinical sample. Neurology. 2018;90:e282–e90.

31. Cho H, Lee HS, Choi JY, Lee JH, Ryu YH, Lee MS, et al. Predicted sequence of cortical tau and amyloid-beta deposition in Alzheimer disease spectrum. Neurobiol Aging. 2018;68:76–84.

32. Jack CR Jr, Knopman DS, Jagust WJ, Petersen RC, Weiner MW, Aisen PS, et al. Tracking pathophysiological processes in

Alzheimer's disease: an updated hypothetical model of dynamic biomarkers. Lancet Neurol. 2013;12:207–16.

33. Crary JF, Trojanowski JQ, Schneider JA, Abisambra JF, Abner EL, Alafuzoff I, et al. Primary age-related tauopathy (PART): a common pathology associated with human aging. Acta Neuropathol. 2014;128:755–66.

34. Duyckaerts C, Braak H, Brion JP, Buee L, Del Tredici K, Goedert M, et al. PART is part of Alzheimer disease. Acta Neuropathol. 2015;129:749–56.